[1]

Design of a radial collimator for the SEQUOIA direct geometry chopper spectrometer

M. B. Stone[a,*], G. Sala[a], J. Y. Y. Lin[a]

[a]*Neutron Scattering Division, Oak Ridge National Laboratory, Oak Ridge, Tennessee 37831, USA*

Abstract

The SEQUOIA direct geometry chopper spectrometer at the Spallation Neutron Source is considering acquisition of a radial collimator. We present here Monte-Carlo calculations examining the proposed collimator's performance. Through comparison of calculations with and without sample environments in place, one can determine appropriate parameters to use in the collimator design. The numerical results provide enough detail to determine the angular collimation for the radial collimator.

Keywords: Inelastic neutron scattering, Collimation, neutron spectroscopy

1. Introduction

Neutron cross sections are relatively small for some metals. This allows one to place samples within complicated sample environments such as cryostats, superconducting magnets, and furnaces during neutron scattering measurements [1]. Although the portion of the sample environment that the neutron beam may traverse is often thinned as much as mechanically possible, there is scattering which occurs due to the sample environment. This is considered part of the background in the measurement, and often needs to be measured separately without the sample in place. Through appropriate collimation of the neutron beam before and/or after the sample and sample environment, this background can be suppressed

*corresponding author

Email addresses: stonemb@ornl.gov (M. B. Stone), salag@ornl.gov (G. Sala), linjiao@ornl.gov (J. Y. Y. Lin)

significantly [2, 3]. This allows for cleaner measurements of the samples and more time to examine the properties of the materials being probed during the measurement. Every good detector deserves a good collimator.

There is currently no incident or scattered beam collimation installed at the SEQUOIA instrument. SEQUOIA is a direct geometry chopper spectrometer at the Spallation Neutron Source (SNS) at the Oak Ridge National Laboratory [4, 5]. It uses an ambient water moderator, and operates with incident energy neutrons between approximately 4 and 6000 meV. SEQUOIA often measures magnetic excitations and lattice/molecular excitations in a variety of materials. These experiments make use of sample environments that contribute to the measured scattering intensity. There are large vertical baffles located in the detector array at SEQUOIA. These start at a radius of approximately 4.25 m from the sample position and extend to the face of the Helium-3 detectors used at SEQUOIA. They are made of boron carbide based material and extend as vertical vanes every approximately 15 degrees within the detector array. Figure 1 shows these baffle positions inside the detector vacuum tank. These baffles serve to suppress detector-detector scattering within the array, but their large distance from the sample position and large angular spacing does not make them efficient collimators of the sample environment.

Using radial collimation after the sample position has been an established method to suppress background scattering due to sample environments at direct geometry spectrometers (DGS) [6, 7, 8, 9, 10, 11, 12]. The thermal DGS instruments at the SNS were designed with the possibility of adding a radial collimator. The ARCS instrument has commissioned a radial collimator [13]. This collimator is most often used when liquid helium cryostats or high temperature furnaces are used as sample environments due to the aluminum shields present in these devices. The collimator at ARCS was designed using analytical expressions for the efficiency of the collimator and comparisons to other collimators used at similar instruments. We present here Monte-Carlo calculations used to determine an appropriate collimation for a radial collimator at the SEQUOIA instrument at the SNS.

2. Collimator boundary conditions

Radial collimators consist of vertical absorbing blades or septa in a radial geometry arranged around the sample position [14]. The blades have an inner, r_1, and outer, r_2, radius measured from the sample position, they are made of a neutron absorbing material and they are as thin as possible to improve transmission of the scattered beam. The angular distance between blades is 2α. For efficient collimation, one would like r_1 to be small, and then one chooses values of r_2 and 2α to appropriately collimate the beam, without reducing too much the transmission of neutrons scattered from the sample. There is also a minimum value of 2α which manufacturers can provide as a function of the radii. The monetary cost of the collimator also needs to be considered in determining these variables.

Important boundary conditions in the collimator design are set by the size of the sample environments used at the instrument and the physical boundaries of the instrument geometry. The SEQUOIA collimator is being designed to use the largest sample environments available at the ORNL facility. This places the collimator in the detector chamber rather

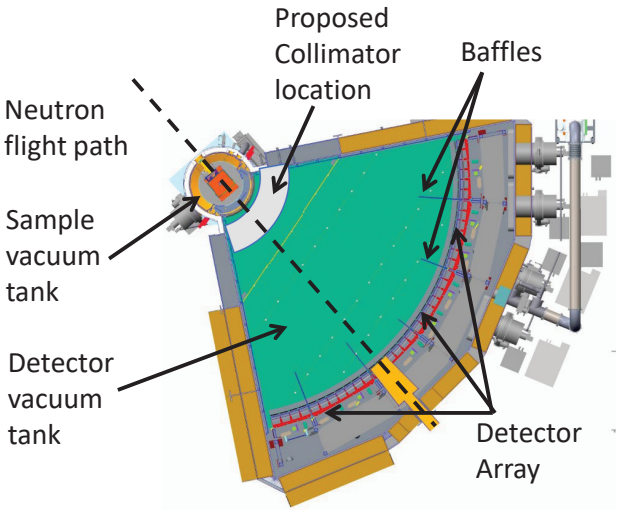

Figure 1: View of the SEQUOIA spectrometer from above the instrument. The incident neutron beam flight path is shown as a dashed line. The proposed radial collimator is placed immediately outside the sample vacuum chamber. A gate valve is in place between the sample chamber and the detector chamber. This gate valve is a load lock mechanism for maintaining cryogenic vacuum in the detector tank when samples or sample environments are changed in the sample chamber.

than the sample vacuum chamber as was done at the ARCS instrument [12]. The opening of the SEQUOIA gate valve is 0.984 m high with an inner radius of 0.724 m from the sample position. However, there is a physical obstruction in the SEQUOIA vacuum chamber that limits the height of the radial collimator. This sets a limit on the outer radius in order to minimize any shadowing of the most upper rows of proposed detector coverage at the instrument. We note that these detectors are not yet installed. With these limits, we choose $r_1 = 819.15$ mm, $r_2 = 1100$ mm, and a height of 1233.5 mm. The total angular range of the collimator will be 87 degrees. This will allow it to completely collimate the angular range of the scattered beam and oscillate about its central position. We also note that to prevent scattering from the incident neutron beam we do not plan to put any collimating vanes within approximately 2.5 degrees of the incident beam. Figure 1 illustrates the location of the radial collimator relative to the other major spectrometer components.

The angular size of each detector tube at SEQUOIA is approximately 0.3° in scattering angle. Single crystal SEQUOIA measurements are often binned by combining two neighboring tubes together to improve signal without any significant loss of wave-vector resolution. This implies that collimating at a level less than 0.6° would be over collimating and reduce beam transmission through the collimator. The ARCS radial collimator blade spacing was chosen in part based upon impact parameter arguments. The incident neutron beam width at SEQUOIA is 50 mm. Measurements very often make use of flat-plate geometry sample cells that completely fill the incident beam. Applying the impact parameter formalism with an impact parameter set to the edge of the incident beam yields a value of $2\alpha = 0.45°$. In practice, the percentage of the scattering volume sampled with a radial collimator will vary linearly from 1 at the beam center to effectively zero at the impact parameter radius.

This would reduce the efficiency of measuring flat plate sample cells. We use Monte Carlo neutron ray tracing methods to determine the optimal blade spacing of the proposed radial collimator to make efficient use of the size of the incident neutron beam while reducing background from sources at larger radii.

3. MCViNE simulations

Monte Carlo neutron ray tracing simulations were performed for a series of radial collimator geometries with different sample and sample environment geometries using MCViNE [15]. MCViNE is designed to model modern neutron instrument components in hierarchy structures, such as detector systems and complex sample environments. All MCViNE simulations performed follow the standard procedure [15] that involves four steps. First, the neutron beam 15 cm upstream of the sample position was simulated. A count of 10^9 neutrons from the thermal moderator were monochromated in the simulation to 100 meV incident energy using the high resolution Fermi chopper available at SEQUOIA. The resulting beam at the sample position was used for all of the calculations. In the second step, the simulated beam was scattered by a virtual sample. The virtual sample was a vanadium rod of 5 mm diameter and 5 cm tall, and it has scattering kernels for vanadium incoherent elastic scattering, incoherent single-phonon and multiphonon inelastic scattering. When sample environment is taken into account, aluminum-made sample environments are included. For simplicity, only coherent and incoherent elastic kernels for aluminum are included. In the third step the interception of simulated scattered neutrons by the SEQUOIA detector system were simulated and NeXus files were generated. In the last step the NeXus files were reduced by Mantid and S(Q,E) spectra were obtained. Figure 2 shows the measured and calculated vanadium inelastic phonon scattering spectra. The overall agreement is good. The radial collimator geometry in the MCViNE calculations used the proposed dimensions listed above with a blade spacing that could be adjusted for the different calculations. The blades were considered infinitely thin and infinitely absorbing of neutrons. The collimator was considered to oscillate about its central location during the course of the simulation. The collimator simulation is done by filtering the neutrons scattered from the sample and sample environment through the collimator component, and the neutrons that pass through the collimator are sent to the virtual detector system for further simulation.

A series of MCViNE simulations were done with a 5 mm diameter vertically oriented vanadium rod. The rod was moved transverse to the incident neutron beam and calculations of the scattering intensity were performed for different collimator blade spacings. The transverse movement of the sample was examined in order to determine the extent of the scattering volume which can be achieved with the collimator in use. Often, flat plate powder samples or large single crystal samples are used at SEQUOIA that effectively fill the width of the incident neutron beam. With the collimator in use, we do not want to significantly reduce the amount of sample material which is effectively scattering. The total scattering intensity as a function of position is shown in Fig. 3. As collimation increases, the effective sample size decreases. For collimation of $2\alpha = 0.4^\circ$ the sampled region of the neutron beam is effectively triangular, and flat plate samples would not be effectively probed with

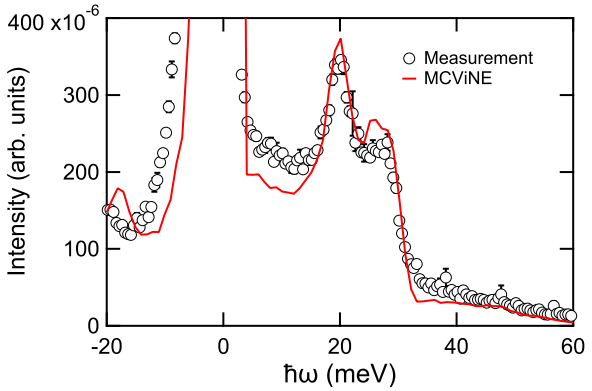

Figure 2: Inelastic neutron scattering spectra of vanadium. Open symbols were measured at SEQUOIA using a 30x30x2 mm vanadium plate using $E_i = 100$ meV neutrons and the higher resolution Fermi chopper. The solid line was calculated using MCViNE for the same sample geometry at the sample position.

such a collimator. Figure 4 shows the integrated calculated scattering intensity for the data in Fig. 3 as a function of blade spacing in the collimator. We compare this intensity to an exponential function, $I = I_0 + A * \exp(-\frac{2\alpha}{\tau})$,and find good agreement with a value of $\tau = 0.434(3)^\circ$. The right axis of Fig. 4 shows the fraction of scattering intensity.

We also consider collimation in the presence of a sample environment. MCViNE calculations were performed with the 5 mm diameter vanadium rod located at the sample center position and a series of 18 cm tall aluminum concentric cylinders surrounding this position. The midpoint of the cylinders were located at the midpoint of the incident beam. The radii and thickness of these cylinders was chosen to match those of a typical liquid helium cryostat used at the SEQUOIA beamline: first shield inner radius 5.045 cm (0.75 mm thick), second shield inner radius 6.66 cm (0.25 mm thick), third shield inner radius 10.636 cm (0.2 mm thick), and outer window inner radius 12.27 cm (0.13 mm thick). Multiple scattering events up to 5 collisions among the sample and aluminum-made sample environments were allowed in the MCViNE calculations. When compared to the calculations with only the vanadium rod in place, these calculations allow one to examine the trade-off between signal and background. Figure 5(a) shows the ratio of integrated scattering intensity calculated with and without the aluminum sample environment in place as a function of collimator spacing. The intensity ratio approaches a value of one as the collimator spacing decreases. At larger values of 2α the background due to the cryostat and multiple scattering between the cryostat and sample is nearly the same scattering intensity as just the sample.

The inset of Fig. 5(a) plots the percentage reduction in background (vertical axis) as a function of the percentage reduction in signal (horizontal axis) due to the vanadium rod. The blade separation value gets smaller as one moves toward the right of this figure. For example, through collimation one can achieve a 38% reduction in background at the expense of a 13% reduction in signal, or for smaller blade separations, one achieves a 95% reduction in background with a 67% reduction in signal. We compare these data to two linear trends. These lines intersect between the points which correspond to $2\alpha = 0.6^\circ$ and $2\alpha = 0.8^\circ$. Blade spacings smaller than $2\alpha = 0.7^\circ$ collimate out background scattering but the signal

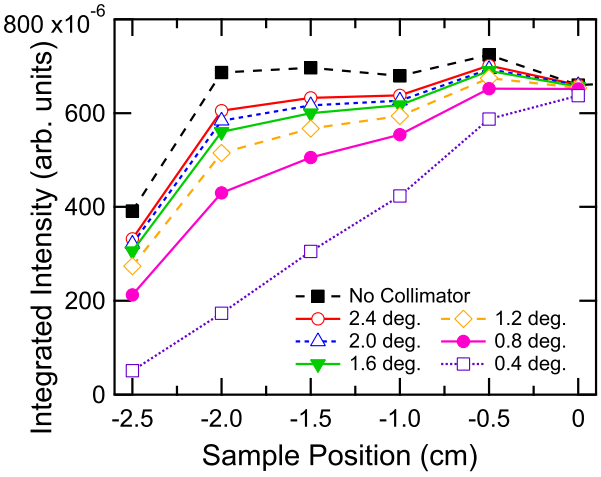

Figure 3: Total calculated scattering intensity as a function of vanadium rod position moving transverse to the incident neutron beam. Different curves were calculated using the blade spacing, 2α, noted in the legend. the x-axis value of zero corresponds to the center of the neutron beam. The x-axis value of -2.5 cm corresponds to the edge of the neutron beam.

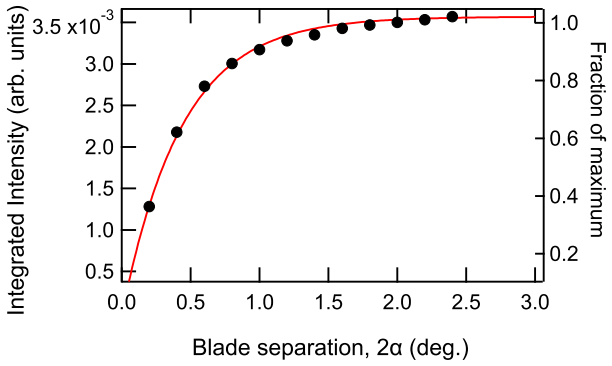

Figure 4: Total calculated scattering intensity as a function of collimator blade spacing. The data were integrated over the calculations of different sample rod positions as shown in Fig. 3. The solid red line is a fit to an exponential as described in the text. The right axis shows the fraction of scattering intensity remaining as one collimates the scattered beam.

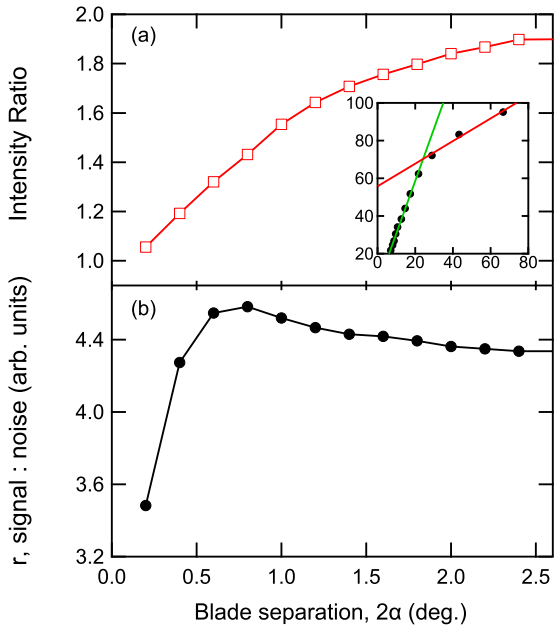

Figure 5: (a) Ratio of calculated scattering intensity with sample environment in place to the scattering intensity without the sample environment in place as a function of collimator spacing, 2α. Both calculations include a vanadium rod at the sample position. (inset) Percentage reduction in background as a function of the percentage reduction in signal. Blade spacing, 2α, gets smaller as one moves toward the right of this figure. (b) Estimate of signal to noise ratio as described in text as a function of 2α.

scattering intensity begins to more rapidly decline.

Another way to consider optimal blade spacing is to examine the signal to noise ratio, r, which can be estimated by observing

$$r = \frac{I}{\sigma} = \frac{I_{sample}}{\sqrt{I_{total}}} \tag{1}$$

where I_{sample} is the scattering intensity from the sample, and I_{total} is the total scattering intensity (including multiple scattering) from the sample and the sample environments. This quantity (scaled by an arbitrary factor) is plotted as a function of 2α in Fig. 5(b). I_{sample} corresponds to the intensity shown in Fig. 4 and I_{total} corresponds to the scattering intensity calculated for the vanadium rod in the center of the aluminum cryostat. This quantity has a local maximum at $2\alpha = 0.8°$.

As an additional point of comparison, we examine the analytic visibility function and figure of merit function that are available for radial collimators. These are fully described in Ref. [14]. The visibility function returns the percentage of the sample that is visible as a function of radius from the beam center, r, and scattering angle, 2θ. Figure 6(a) and (b) plot the calculated visibility as a function of scattering angle (horizontal axis) and radius from the sample position (vertical axis) for (a) no radial collimator in position and (b) a 0.8 degree blade separation radial collimator. For these calculations, the center of the incident

beam is at 0 and the edge of the beam is at a radius, $r = 25$ mm. Figure 6(a) effectively shows the visibility in the absence of any secondary collimation, and Fig. 6(b) illustrates that the proposed radial collimator will reduce scattering outside the 25 mm width of the incident neutron beam. Figure 6(c) shows the figure of merit for the proposed SEQUOIA radial collimator as a function of scattering angle in comparison to the ARCS and HYSPEC radial collimators. The figure of merit compares well with the existing collimators.

4. Conclusions

We examine neutron ray-tracing Monte Carlo calculations for the SEQUOIA instrument using different radial collimators in the scattered beam. The scattering kernels include a vanadium rod at the sample position and moving transverse to the incident beam, as well as the vanadium rod centred in cylindrical aluminum shells approximating a liquid helium cryostat. We find that for samples which will fill the incident beam at SEQUOIA, the blade separation should be $2\alpha \geq 0.8^\circ$ to achieve at least an 80% measure of the scattering volume as shown in the right axis of Fig. 4. We also find that the trend in percent reduction in background versus the percent reduction in signal changes abruptly for values of $2\alpha \leq 0.7^\circ$: such values over collimate the background at the expense of measuring the signal. Last of all, we find that there is a peak in the ratio of calculated signal scattering to that of the background for values of $2\alpha \approx 0.8^\circ$. These three comparisons suggest that a value of blade spacing of $2\alpha = 0.8^\circ$ is appropriate for a SEQUOIA radial collimator. We note that the calculations assume that the blades have no thickness. In the built collimator, these blades will have a thickness. The finite thickness of the blades will reduce the transmission of the collimator. To account for this, we suggest that the SEQUOIA radial collimator be built with a slightly larger minimum blade spacing of $2\alpha = 0.9^\circ$.

5. acknowledgments

This work was supported by the U.S. DOE, Office of Science, Basic Energy Sciences, Materials Sciences and Engineering Division. This research used resources at the High Flux Isotope Reactor and Spallation Neutron Source, DOE Office of Science User Facilities operated by the Oak Ridge National Laboratory.

References

[1] I. F. Bailey, A review of sample environments in neutron scattering., Z. Kristallogr. 218 (2003) 84–95. doi:https://doi.org/10.1524/zkri.218.2.84.20671.

[2] W. Soller, A new precision x-ray spectrometer., Phys. Rev. 24 (1924) 158–167. doi:https://doi.org/10.1103/PhysRev.24.158.

[3] C. Carlile, P. Hey, B. Mack, High-efficiency soller slit collimators for thermal neutrons., J. Phys. E: Sci. Instrum. 10 (1977) 543–546. doi:https://doi.org/10.1088/0022-3735/10/5/035.

[4] G. E. Granroth, A. I. Kolesnikov, T. E. Sherline, J. P. Clancy, K. A. Ross, J. P. Ruff, B. D. Gaulin, S. E. Nagler, Sequoia: a newly operating chopper spectrometer at the sns., Journal of Physics: Conference Series 251 (2010) 12058. doi:https://doi.org/10.1088/1742-6596/251/1/012058.

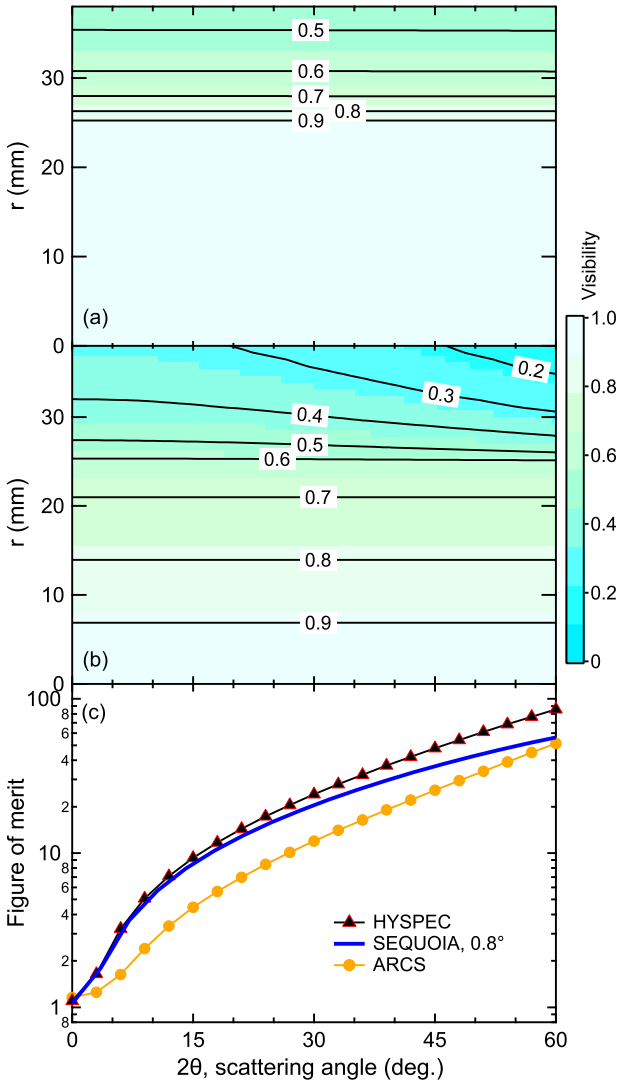

Figure 6: Visibility and figure of merit as a function of scattering angle, 2θ. (a) Visibility as a function of scattering angle (horizontal axis) and radius from sample center (vertical axis) for a radial collimator with 90 degrees between blades. (b) Visibility as a function of scattering angle (horizontal axis) and radius from sample center (vertical axis) for a radial collimator with 0.8 degrees between blades. (c) Figure of merit as a function of scattering angle for the proposed SEQUOIA radial collimator in comparison to the HYSPEC and ARCS radial collimators. Calculation was done using the entire available beam width of the corresponding instruments.

[5] M. B. Stone, J. L. Niedziela, D. L. Abernathy, L. DeBeer-Schmitt, G. Ehlers, O. Garlea, G. E. Granroth, M. Graves-Brook, A. I. Kolesnikov, A. Podlesnyak, B. Winn, A comparison of four direct geometry time-of-flight spectrometers at the spallation neutron source., Review of Scientific Instruments 85 (2014) 045113. doi:https://doi.org/10.1063/1.4870050.

[6] J. Mesot, S. Janssen, L. Holitzner, R. Hempelmann, Focus: Project of a space and time focussing time-of-flight spectrometer for cold neutrons at the spallation source sinq of the paul scherrer institute., Journal of Neutron Research 3 (4) (1996) 293–310. doi:https://doi.org/10.1080/10238169608200202.

[7] J. R. D. Copley, J. C. Cook, The disk chopper spectrometer at nist: a new instrument for quasielastic neutron scattering studies., Chemical Physics 202 (2-3) (2003) 477–485. doi:https://doi.org/10.1016/S0301-0104(03)00124-1.

[8] T. Unruh, J. Neuhaus, W. Petry, The high-resolution time-of-flight spectrometer toftof., Nucl. Instrum. Methods Phys. Res. A 580 (2007) 1414. doi:https://doi.org/10.1016/j.nima.2007.07.015.

[9] G. Ehlers, A. A. Podlesnyak, J. L. Niedziela, E. B. Iverson, , P. E. Sokol, The new cold neutron chopper spectrometer at the spallation neutron source: Design and performance., Review of Scientific Instruments 82 (2011) 085108. doi:https://doi.org/10.1063/1.3626935.

[10] J. Ollivier, H. Mutka, In5 cold neutron time-of-flight spectrometer, prepared to tackle single crystal spectroscopy., J. Phys. Soc. Jpn. 80 (2011) SB003. doi:https://doi.org/10.1143/JPSJS.80SB.SB003.

[11] D. Yu, R. Mole, T. Noakes, S. Kennedy, R. Robinson, Pelicana time of flight cold neutron polarization analysis spectrometer at opal., J. Phys. Soc. Jpn. 82 (2013) SA027. doi:https://doi.org/10.7566/JPSJS.82SA.SA027.

[12] M. B. Stone, J. L. Niedziela, M. J. Loguillo, M. A. Overbay, D. L. Abernathy, A radial collimator for a time-of-flight neutron spectrometer., Review of Scientific Instruments 85 (2014) 085101. doi:https://doi.org/10.1063/1.4891302.

[13] M. Stone, J. Niedziela, M. Overbay, D. Abernathy, The arcs radial collimator., EPJ Web of Conferences 83 (2015) 03014. doi:https://doi.org/10.1051/epjconf/20158303014.

[14] J. R. D. Copley, J. C. Cook, An analysis of the effectiveness of oscillating radial collimators in neutron scattering applications., Nucl. Instrum. Methods Phys. Res. A 345 (1994) 313–323. doi:https://doi.org/10.1016/0168-9002(94)91008-1.

[15] J. Y. Y. Lin, H. L. Smith, G. E. Granroth, D. L. Abernathy, M. D. Lumsden, B. Winn, A. A. Aczel, M. Aivazis, B. Fultz, Mcvine an object oriented monte carlo neutron ray tracing simulation package., Nuclear Instruments and Methods in Physics Research Section A: Accelerators, Spectrometers, Detectors and Associated Equipment 810 (2016) 86–99. doi:https://doi.org/10.1016/j.nima.2015.11.118.